Solid State Science and Technology, Vol. 32, No. 2 (2024) 152-162
https://doi.org/10.66514/ssst32-2-152-162

DFT Study of the Cation Distribution on Stability, Structural and Electronic Properties of Ni-Doped Spinel Co_3O_4

Nur Hamizah Mohd Zaki[1,2], Ainnur Sherene Kamisan[1,2], Rosnah Zakaria[1,2], Nor Kartini Jaafar[1,2], Fadhlul Wafi Badrudin[3], Mohamad Fariz Bin Mohamad Taib[1,2], Oskar Hasdinor Hassan[3,4], Ab Malik Marwan Ali[1,2]

[1]*Faculty of Applied Sciences, Universiti Teknologi MARA, 40450 Shah Alam, Malaysia*

[2]*Ionic Materials and Devices (iMADE), Institute of Sciences, Universiti Teknologi MARA 40450 Shah Alam, Selangor, Malaysia*

[3]*Faculty of Defense Science and Technology, Universiti Pertahanan Nasional Malaysia, 57000 Kuala Lumpur, Malaysia*

[4]*Department of Industrial Ceramic, Faculty of Art and Design, Universiti Teknologi MARA, 40450 Shah Alam, Selangor, Malaysia*

***** *Corresponding author; email: hamizahzaki@uitm.edu.my*

Received: 22 August 2024 / Accepted: 26 November 2024

ABSTRACT

The origin of spinel cobaltite properties can be attributed to the cation distribution between tetrahedral and octahedral coordination. The choice of spinel types is primarily considered due to the different octahedral and tetrahedral crystal fields where the degeneration of the 3*d* orbital is different and could lead to dissimilar electronic properties. In this work, a theoretical study based density functional theory (DFT) by using CASTEP was performed on Ni-doped Co_3O_4 ($NiCo_2O_4$) to explore the structural, magnetic and electronic properties. From the computed inversion energy and formation energy study, the resulting $NiCo_2O_4$ is energetically favorable in inverse spinel type where Ni prefers to substitute with Co at the octahedral site. The result revealed that the substitution of Ni cation has substantially changed the structure from cubic to tetragonal due to the elongation of the Ni-O bonding at the octahedral site which caused Jahn-Teller (JT) distortion. DOS results showed that $NiCo_2O_4$ has transformed from semiconductor Co_3O_4 into half-metallic material as seen in the spin-down channel which crossed the Fermi level. In addition, details of octahedral crystal field splitting have demonstrated the reason for Jahn-Teller distortion in $NiCo_2O_4$.

Keywords: Density functional theory; spinel Co_3O_4; doping; electronic properties; magnetic properties

INTRODUCTION

In recent times, transition metal oxides (TMOs) have attracted vast attention as electrode material for use in energy storage devices e.g., batteries and supercapacitors due to its high electron storage capability and emissivity through a chemical redox reaction [1,4]. Intensive

studies were conducted on cost-effective TMOs including the spinel cobaltite of cobalt oxide, Co_3O_4. The excellent chemical behaviour and controllable nanostructures of Co_3O_4 are the interesting features that are suitable for an electrode material [5,6,7]. Nevertheless, Co_3O_4 suffers from slow electrochemical reaction kinetics and poor electrical conductivity which affected to electrochemical performance of rate capabilities and cycling stability [8]. These drawbacks are also causing problems in reaching the high theoretical specific capacitance of Co_3O_4 (3000-3900 Fg^{-1}). The emerging use of Co_3O_4 doping with other compatible metals to form binary oxide which enhance the conductivity of Co_3O_4 consequently give good impact on the performance of energy storage devices [9,10]. The binary metal oxide of spinel cobaltite, $M_xCo_{3-x}O_4$ (M=metal) can be prepared via doping with the other metal into Co_3O_4. Generally, a similar ionic radius of doping metal with host ion may give an effective enhancement on its properties [11]. Researchers has performed both experimental and theoretical work stated above and among metals (*M*=Ni, Zn and Mn) Ni doping showed the lowest band gap and becomes more conductive than others [12,13]. It is consistent with other work where Ni substitution for Co atom to obtained $NiCo_2O_4$ yielded a lower band gap and greater density of states near the Fermi surface [14].

Theoretically, the crystal structure of the doped Co_3O_4 depends on the cation distribution which strongly affected the cation-anion bonding, magnetic properties and band structure. The spinel structure of $M_xCo_{3-x}O_4$ is arranged in face-centered cubic (FCC) where the cations have two sites to occupy either tetrahedral (8a) or octahedral sites (16*d*). By depending on the cation distribution, the normal structure is referred to as Co atoms occupying a tetrahedral site meanwhile *M* (doping atoms) occupy octahedral sites. For inverse structure, the Co atoms are distributed over both tetrahedral and octahedral sites while *M* (doping atoms) occupy the octahedral sites. The cation distribution is strongly influenced the lattice parameter, Mulliken population analysis and the electronic properties [15]. Besides that, it can also cause magnetic frustration or enhanced magnetic interaction [16]. So a clear understanding of the cation distribution in spinel cobaltite is essential for studying and controlling their properties. A better relationship between them need to be established so that the properties of spinel cobaltite can be easily tuned just by varying the distribution of cations at A and B sites [17], [18]. A comprehensive study of fundamental understanding on the material is also important to design a new electrode material by studying the theoretical work. Currently, the density functional theory (DFT) has gained recognition because it is a powerful tool in predicting the properties of various materials including metal oxides. This work is focused on investigating the binary oxide of spinel cobaltite of $NiCo_2O_4$ by substituting Co in Co_3O_4 at different site (tetrahedral or octahedral) with Ni by using DFT calculation. The analysis on the structural and electronic properties of $NiCo_2O_4$ depending on the cation distribution were considered in this work.

COMPUTATIONAL DETAILS

All calculations were performed using Cambridge Serial Total Energy Package (CASTEP) implemented in Material Studio based on density functional theory (DFT). The DFT calculations were treated within semi-local generalized gradient approximation (GGA) exchange-correlation functional of the Perdew-Burke-Ernzerhof for solids (PBEsol) [19]. The ultrasoft pseudopotential were used to model valence-electron interactions while O $2s^22p^4$, Co $3d^74s^2$, and Ni $3d^84s^2$ were considered as valence electron configuration. The plane wave cut off was chosen to be 380eV to ensure acceptable precision and 4×4×4 k-point grids were used in the geometry optimization of the bulk structure. The density mixing parameters of charge density mixing amplitude, cut-off energy for mixing and charge density mixing g-vector were 0.5000, 300.0 eV and 1.5001 A-1, respectively. The Hubbard U

correction employed for Co 3*d* orbitals is 4 eV and 6.3 eV for Ni 3d orbital corresponds to the previous study on NiO [30]. It is set for the spin state at tetrahedral site occupied by high spin (HS) Co^{2+} (S=3/2), Co^{3+} (S=2) while at the octahedral site occupied by low spin (LS) Ni^{3+} (S=1/2), Co^{3+} (S=0) and (HS) Ni^{2+} (S=1). The details of spin ordering for each cation are shown in Table 1. The formation of Ni doped Co_3O_4 is made by substitution of metal doping with Co-host atoms. From Co_3O_4 structure, 8 Co atoms are substituted with Ni atoms at two different sites. Based on the cation distribution, the spinel type has the general formula of AB_2O_4 to form a normal spinel structure meanwhile with the formula $B[AB]O_4$ to form inverse spinel structure. So, taken into consideration, the calculations were performed with cation distribution, *x* where *x*=0 (normal) and *x*=1(inverse) to determine the stability of structure.

Table 1. The spin ordering for 3d metal according to the cation distribution

Material	Inversion degree, *x*	Tetrahedral- site		Octahedral-site	
		Formula unit	Spin ordering	Formula unit	Spin ordering
$NiCo_2O_4$	0	(Ni^{2+})	↑↑↑↑↓↓↓↓	$[Co^{3+}]$	None
	1	(Co^{2+})	↑↑↑↑↓↓↓↓	$[Ni^{3+}Co^{3+}]$	Ni^{3+}- ↓↓↓↓↓↓↓↓ Co^{3+}- None

RESULTS AND DISCUSSION

Structural Properties

It is acknowledged that the spinel structure can be divided into two types i.e., normal and inverse spinel which correspond to the cation distribution in the multivalence atom. With that, via first principle study we determined the site preference of cation distribution to obtain the stable structure by calculating the energy difference of normal and inverse structure [19]. Here,

$$\Delta E = E(inverse) - E(normal) \qquad (1)$$

where ΔE is the differences of energy of spinel in normal (*x*=0) and inverse (*x*=1). Other than that, the formation energy is calculated in order to predict the energy required to form the compound and relative stability. The formula of impurity formation energy is referred to the formalism defined by Van de Walle et al. [20]. The formation energy was calculated using the following expression:

$$E_f = E_{M:Co_3O_4} + E_{Co} - (E_{Co_3O_4} + E_M) \qquad (2)$$

where $E_{M:Co_3O_4}$ is the total energy of *M*-doped Co_3O_4, $E_{Co_3O_4}$ is the total energy of pure Co_3O_4 and E_M and E_{Co} represent the energy of single *M* atom and Co atom, respectively. The calculated formation energy for $NiCo_2O_4$ with different cation distributions is tabulated in Table 2. The lowest formation energy obtained is at *x*=1. Hence indicates $NiCo_2O_4$ is energetically favorable in inverse structure. The experimental work by Lenglet et al., [21] using EXAFS spectra has proved the occurrence of Ni element at the octahedral site instead of occupying the tetrahedral site.

Table 2. The formation energy of the different cation distribution for $NiCo_2O_4$

Material	Total energy (eV)			Impurity formation energy (eV)
		$E_{Co_3O_4}$	E_{Co}	
Co_3O_4		-38848.159	-1034.761	
	Cation distribution, x	$E_{M:Co_3O_4}$	E_M	E_f
$NiCo_2O_4$	0	-41438.761	-1347.149	-2278.210
	1	-41481.951		-2321.404

The geometry optimization was performed to the inverse spinel $NiCo_2O_4$ according to the more stable structure. For $NiCo_2O_4$, the inverse spinel structure, Ni cation occupy half of the octahedral site and Co atom is distributed over octahedral and tetrahedral site as displayed in

Figure 1. The trivalent cation Co^{3+} and Ni^{3+} are octahedrally (B) bounded by six oxygen atoms, whereas divalent cation Co^{2+} (A) is tetrahedrally surrounded by four oxygen. The formula for $NiCo_2O_4$ can be expressed as $(Co^{2+})[Ni^{3+}Co^{3+}]O_4$. From the optimized structure of $NiCo_2O_4$, the calculated lattice parameter (*a*), unit cell volume (*V*) and anion displacement parameter (*u*) with comparison with Co_3O_4 are listed in

Table 3. It is noticeable that the lattice parameter of $NiCo_2O_4$ has changed from cubic to tetragonal mainly the alteration in elongated along the c-direction. The calculated lattice parameter for $NiCo_2O_4$ is higher than the calculated Co_3O_4 by (*a, b* =+1.63%, *c* = +1.74%). There is an elongation that can be explained resulting from Ni-O bond expansion related to the Jahn-Teller (JT) effect with the c/a ratio of 1.0. The Jahn-Teller distortion is due to unsymmetrical arrangement of Ni^{3+} in orbital at octahedral thus leading to maximum stability of a particular octahedral complex [22], [23]. In order to better illustrate, the local atomic structure of NiO_6 is shown in Figure 2 which is identified as predominantly influence in the local distortion. It seems Ni-O bond length is slightly elongated to 2.00 Å along the *z*-axis while other bonds are in 0.99 Å. Although the differences in calculated bond length seem small, still the distortion of Ni^{3+}-O_6 bond lengths is mainly responsible for the changes in lattice parameter and rise the crystal volume by 5.11% compared to undoped Co_3O_4. Some of the studies based on $NiCo_2O_4$ found this material exhibited in cubic structure which is contradictory to this work [14]. This is due to the differences of site preference and the cation arrangement of Ni and Co gives tendency on any changes in the structure. For $NiCo_2O_4$, the magnetic moment for Ni is -0.78μ_B and for Co is 2.47μ_B contributed by the Ni^{3+} (octahedral site) and Co^{2+} (tetrahedral site), respectively. It is in good agreement with other theoretical studies [24] and also with the experimental value obtained -1.49 μ_B for Ni and 2.18 μ_B for Co [25].

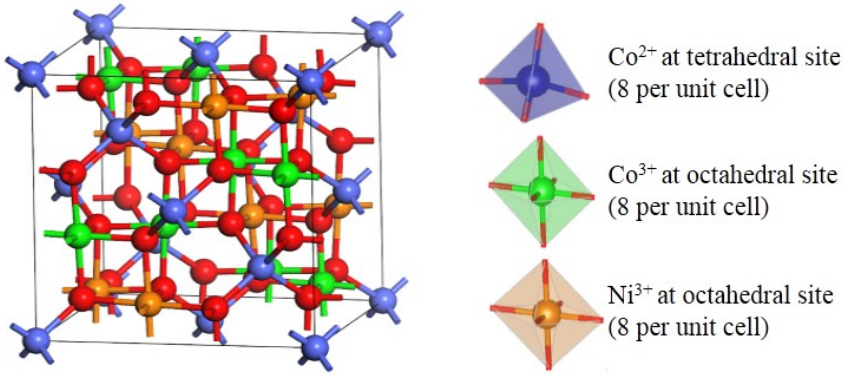

Figure 1. Crystal structure of inverse spinel $NiCo_2O_4$. The green ball represent Co atom and orange ball represents Ni atom, respectively

Table 3. Structural parameters, unit cell volumes (V) and anion displacement (u) of $NiCo_2O_4$. Values in the parentheses represent percentage differences with undoped Co_3O_4

Material		Lattice parameter (Å)			Volume (V)	u
		a	b	c		
Co_3O_4	This work	8.087	8.087	8.087	528.984	-
	Other theoretical GGA-PBE [26]	8.190	8.190	8.190	549.35	
	GGA-PBE [27]	8.110	8.110	8.110	-	
	Experimental Ref.[28][a]	8.084	8.084	8.084	528.32	
	Ref.[29][b]	8.067	8.067	8.067	-	
$NiCo_2O_4$	This work	8.219 (+1.63%)	8.219 (+1.63%)	8.228 (+1.74%)	555.993 (+5.11%)	0.261

[a]X-Ray diffraction analysis samples at ambient pressure
[b]X-Ray diffraction analysis samples prepared by hydrothermal method

From the structural properties, the investigation on the stability of structure between normal vs spinel of $NiCo_2O_4$ also can be further confirmed by analyzing the anion displacement (u) obtained from the atomic coordinate. Stevanovic et al. has proposed the model for (2-3 or 4-2 spinel) [30,31,32]. For this work the 2-3 spinel is applicable which indicates the nominal charge involved in the material. The rules are stated in order to differentiate the model of the structure by using the general formula A_2BO_4 and nominal charge of species (Z) where $Z_A > Z_B$, the normal structure is preferred if $u > 0.2592$ and inverse structure is preferred if $u < 0.2578$. For $Z_A < Z_B$, normal structure is preferred if $u < 0.2550$ and inverse structure is preferred if $u > 0.2578$. The equation used to determine the u value and the rules proposed is simplified in the equation:

$$\boldsymbol{d = a\sqrt{3}\left(u - \frac{1}{8}\right)} \qquad (3)$$

where the u is derived from the distance between tetrahedral cation and the anion and a is lattice constant. For $NiCo_2O_4$ it is obtained the $Z_A < Z_B$ with $u = 0.261$ indicates favorable

in inverse structure. Hence, from this prediction it is made firm that the stable structure for $NiCo_2O_4$ is unambiguously in the inverse spinel structure.

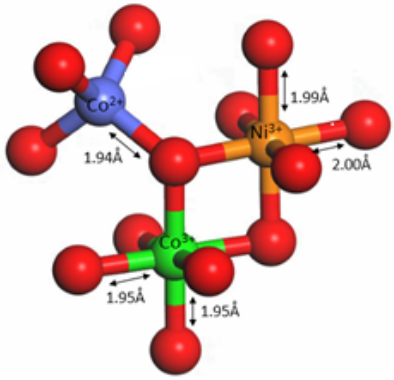

Figure 2. The cation-anion bond length of $NiCo_2O_4$

Electronic Properties

The effect of doping material can lead to significant changes in the electronic properties of band structure and density of states (DOS). By perceiving the band structure can signify its properties and may potentially know the material characteristics. Figure 4 demonstrates the band structure along the symmetry points (W-L-G-X-W-K). It is seen at the majority spin of $NiCo_2O_4$, the narrower band gap of 1.40 eV along the (G-X) and 1.54 eV at (X-X) direction compared to undoped Co_3O_4 (1.69 eV) (Figure 3) meanwhile the strong dispersion occurs at minority spin and has across the Fermi level. This verifies that $NiCo_2O_4$ has turned the semiconductor into half-metallic material. The relatively small band gap at majority spin is feasible for thermal excitations to raise electrons to the conduction band hence exhibits higher electrical conductivity. At the minority spin, the metallic behaviour is contributed by the e_g and t_{2g} orbitals of Ni (octahedral site) and Co (tetrahedral site). Thus, the exchange interaction could occur between Ni and Co which greatly influence the electrical conductivity of $NiCo_2O_4$ [24]. The higher electrical conductivity is consistent with experimental data where $NiCo_2O_4$ showed an increased of at least two orders of magnitude compared to undoped Co_3O_4 [33]. This result of the band diagram contradict with Zhu et al., who studied on normal spinel $NiCo_2O_4$ which found that the band diagram is just like a typical semiconductor band structure [14]. This dissimilarity gives rise to the belief that the cation distribution plays a crucial role in electronic properties modification.

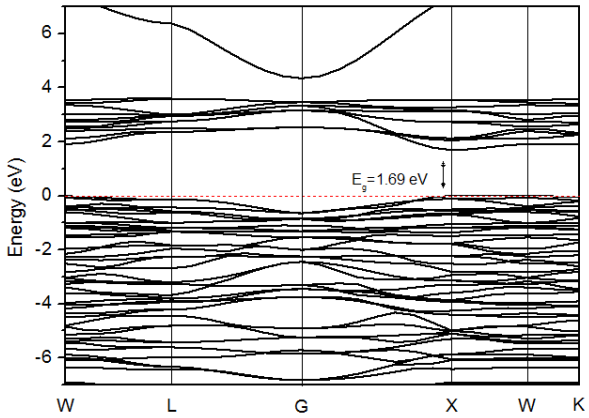

Figure 3. Band structure of Co_3O_4. The Fermi level is set to zero

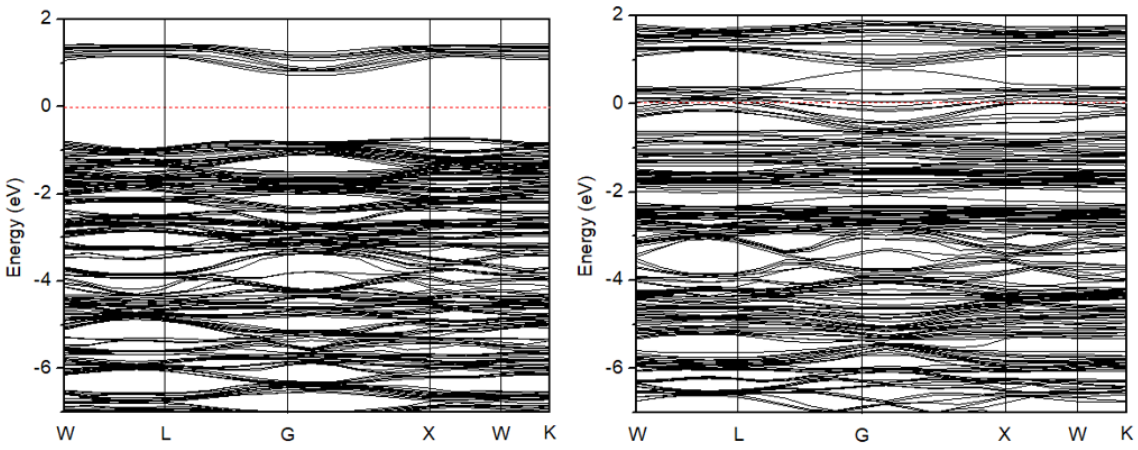

Figure 4. Band structure of $NiCo_2O_4$ in majority spin channel (left) and minority spin channel (right). The Fermi level is set to zero

To gain a better insight into the orbital contributions to electronic bands, the density of states of $NiCo_2O_4$ is analyzed. Figure 5 presents the total and partial density of states of $NiCo_2O_4$ in the majority (spin up) and minority spin (spin down). At spin up the channel remains existed a semiconductor gap with smaller band gap (1.40 eV) meanwhile at spin down the channel has crossed the Fermi level which indicates via Ni doping could transform from semiconductor Co_3O_4 into half-metallic material. From partial densities of states (PDOS), the spin down channel located exactly at the Fermi level region are primarily contributed from Co 3*d*, Ni 3*d* and O 2*p* states. This is attributed to the partially occupied e_g and t_{2g} orbital for Ni 3*d* and Co 3*d*, respectively with the presence of a significant hybridization between cation 3*d* and oxygen 2*p* orbitals. Thus, the exchange interaction within Ni (octahedral) and Co (tetrahedral) may take place and influence the good conductivity in this material. Thus, it is verified that the substitution of Co^{3+} with Ni^{3+} has tremendously altered the electronic properties suggesting the improvement of electrical conductivity for the electrode material.

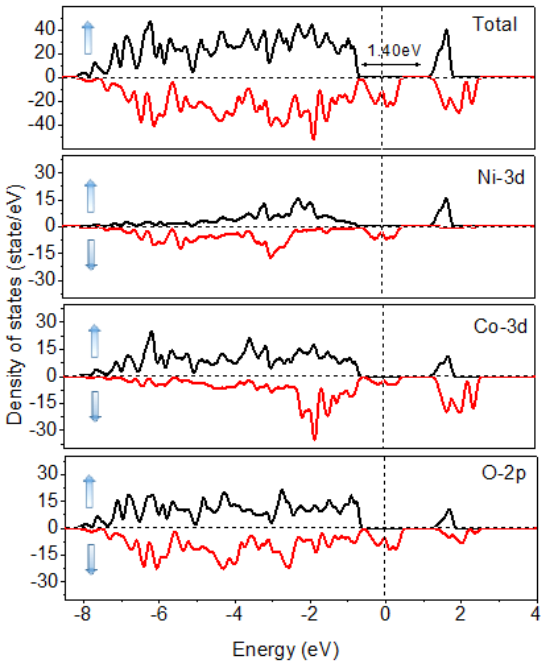

Figure 5. Total and partial density of states (DOS) of $NiCo_2O_4$. The spin states up (↑) and down(↓) are given for details electronic properties

The crystal field splitting used to demonstrate the *d* orbitals degeneracy is broken due to the static electric field. Figure 6 shows the schematic diagram of crystal field splitting in Co 3*d* (Co^{2+} and Co^{3+} ions) and Ni $^{3+}$ ion in $NiCo_2O_4$. For Co^{2+}, the electron is doubly occupied at e_g orbitals and partly fill the t_{2g} orbital. Meanwhile Co^{3+} ions fully occupied the t_{2g} orbital. Therefore, the configuration of Co^{3+} ions with the spin state is ($t_{2g}^6 e_g^0$) and Co^{2+} ions are ($e_g^4 t_{2g}^3$) . Regarding to the Jahn-Teller distortion of $NiCo_2O_4$, specification on the Ni 3*d* is presented at e_g orbital and triplet t_{2g} orbital in the spin up channel to understand the splitting of unsymmetrical arrangement. The e_g orbits in the spin up channel atoms are further split, which brings down the Ni d_{z2} orbits and opens a gap of about 1.40 eV between the Ni d_{z2} and the Ni d_{x2-y2}. The lowered d_{z2} orbits become filled and the corresponding Ni atoms become Ni^{3+}, which is JT active.

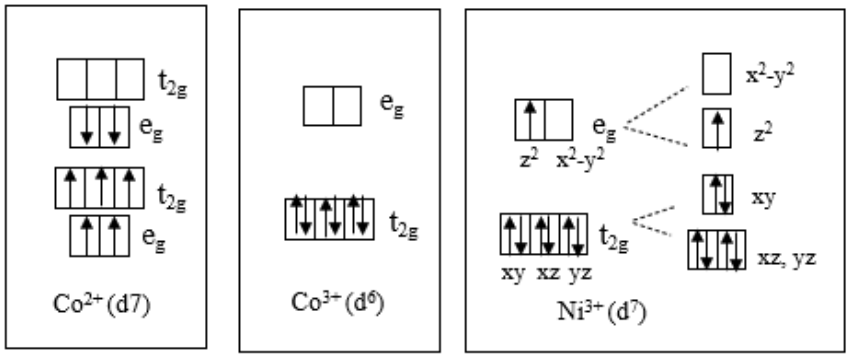

Figure 6. Schematic diagram for 3*d* level splitting in the crystal field theory of $NiCo_2O_4$ with details splits of Ni 3*d* states due to Jahn Teller effect

The information on the nature of chemical bonding among Co-O, Ni-O and Zn-O can be studied from the plot of electron density map [34]. Figure 7 illustrates the electron density map of $NiCo_2O_4$ at {110} plane with the range of the field value. The variation in the color of the centre of the atom indicates the electron density where reddish is more concentrated to blue as it diminishes. Electron distribution changes because of the formation of covalent bonds. As stated in DOS analysis, the presence of hybridization of 3*d* states and O 2*p* states can form a bonding between them. Thus, it is observed for $NiCo_2O_4$ the appearance of covalence bonding of Ni^3 and Co^{2+} with O anion.

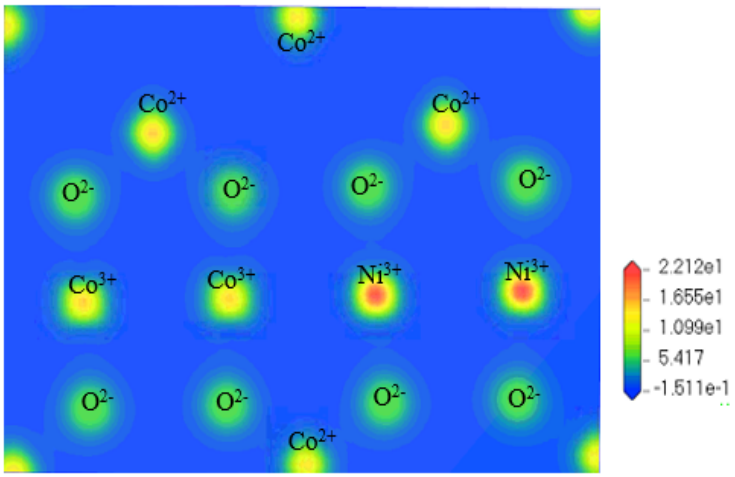

Figure 7. Electron density map of $NiCo_2O_4$ at {110} plane

CONCLUSIONS

In spinel structure, it is important to consider the cation distribution specifically involving the substitution of any cation in the metal oxide. It is vital to elucidate cation distribution because it can lead to different electronic properties. From the computed inversion energy and formation energy resulting to the $NiCo_2O_4$ is energetically favorable in inverse spinel. The substitution of Co cation with Ni has substantially changed the structural parameter and the elongation of the *M*-O bonding at the octahedral site of $NiCo_2O_4$ which caused the Jahn-Teller distortion due to degeneracy breaking by the stabilization (lowering energy) of *d* orbitals. DOS also has verified that $NiCo_2O_4$ has turned into half-metallic material due to minority spin across the Fermi level. The details on octahedral crystal field splitting of $NiCo_2O_4$ have proven the reason for Jahn-Teller effect to occur in $NiCo_2O_4$.

ACKNOWLEDGMENTS

This work is supported by the Ministry of Education (MOE) under the Fundamental Research Grant Scheme (600-RMC/FRGS 5/3 (055/2022). The authors would like to thank to Universiti Teknologi Mara (UiTM) and Ionics, Materials, and Devices (iMADE) Research Laboratory, Institute of Science (IOS) for their support in providing research facilities for this research.

REFERENCES

[1] T. Kim (2022). Implication of magnetic property on the degradation process of layered Ni-rich transition metal oxide cathode for high-capacity lithium-ion batteries, *J. Magn. Magn. Mater.* **564**, 170107

[2] M. Mustaqeem, G. A. Naikoo, M. Yarmohammadi, M. Z. Pedram, H. Pourfarzad, R. A. Dar, S. A. Taha, I. U. Hassan, M. Y. Bhat, Y. Chen (2022). Rational design of metal oxide based electrode materials for high performance supercapacitors – A review, *J. Energy Storage* **55**, 105419.

[3] I. Ibrahim, S. Zheng, C. Y. Foo, N. M. Huang, and H. N. Lim （2021）. Hierarchical nickel-based metal-organic framework/graphene oxide incorporated graphene nanoplatelet electrode with exceptional cycling stability for coin cell and pouch cell supercapacitors, *J. Energy Storage* **43**, 103304.

[4] A. V. Khramenkova, V. V. Moshchenko, A. A. Yakovenko, K. A. Pushnitsa, A. A. Pavlovskii, and M. Y. Maximov (2022). Synthesis, structure investigation and future prospects of transition metal oxides/carbon cloth hybrids as flexible binder-free anode materials for lithium- ion batteries, *Mater. Lett.* **329**, 133250.

[5] F. Gu, C. Li, Y. Hu, and L. Zhang (2007). Synthesis and optical characterization of Co3O4 nanocrystals, *J. Cryst. Growth* **304**, 369.

[6] G. X. Pan *et al.* (2014). High-performance asymmetric supercapacitors based on core / shell cobalt oxide / carbon nanowire arrays with enhanced electrochemical energy storage, *Electrochim. Acta* **133**, 522.

[7] M. B. Durukan, R. Yuksel, H. E. Unalan (2016) Cobalt Oxide Nanoflakes on Single Walled Carbon Nanotube Thin Films for Supercapacitor Electrodes, *Electrochim. Acta* **222**, 1475.

[8] T. Wang, H. C. Chen, F. Yu, X. S. Zhao, H. Wang (2019). Boosting the cycling stability of transition metal compounds-based supercapacitors, *Energy Storage Mater.* **16**, 545.

[9] D. P. Dubal, P. Gomez-Romero, B. R. Sankapal, R. Holze (2015). Nickel cobaltite as an emerging material for supercapacitors: An overview, *Nano Energy* **11**, 377.

[10] D. Zhang *et al.* (2016). Self-assembly of mesoporous $ZnCo_2O_4$ nanomaterials: density functional theory calculation and flexible all-solid-state energy storage, *J. Mater. Chem. A* **4**(2) 568.
[11] Souraya Goumri-Said, Wilayat Khan, Karem Boubaker, G. Turgut, E. Sönmez, Jan Minar, Mohamed Bououdina, Mohammed Benali Kanoun (2019). Europium incorporation dynamics within NiO films deposited by sol-gel spin coating: Experimental and theoretical studies, *Mater. Res. Bull.* **118**, 110525.
[12] H. Adhikari, D. Neupane, C.K. Ranaweera, J. Candler, R. K. Gupta, S. Sapkota, X. Shen, S.R. Mishra (2016). Template-free synthesis of hierarchical mixed-metal cobaltites: Electrocapacitive and Theoretical study, *Electrochim. Acta* **225**, 514.
[13] S. A. Ansari, S. Goumri-Said, H. M. Yadav, M. Belarbi, A. Aljaafari, M. B. Kanoun (2021). Directly grown of $NiCo_2S_4$ nanoparticles on a conducting substrate towards the high-performance counter electrode in dye-sensitized solar cell: A combined theoretical and experimental study, *Sol. Energy Mater. Sol. Cells* **225**, 111064.
[14] Y. Zhu, X. Ji, Z. Wu, W. Song, H. Hou, Z. Wu, X. He, Q. Chen, C.E. Banks (2014). Spinel NiCo2O4 for use as a high-performance supercapacitor electrode material: Understanding of its electrochemical properties, *J. Power Sources* **267**, 888.
[15] S. Liu, D. Ni, H.-F. Li, K. N. Hui, C.-Y. Ouyang, S. C. Jun (2018). Effect of cation substitution on the pseudocapacitive performance of spinel cobaltite MCo_2O_4 (M = Mn, Ni, Cu, and Co), *J. Mater. Chem* **00**, 1.
[16] G. Kumar, R.K. Kotnala, J. Shah, V. Kumar, A. Kumar, P. Dhiman, M. Singh (2017). Cation distribution: A key to ascertain the magnetic interactions in a cobalt substituted Mg-Mn nanoferrite matrix, *Phys. Chem. Chem. Phys.* **19**(25), 16669.
[17] X.C. Huang, J.Y. Zhang, M. Wu, S. Zhang, H.Y. Xiao, W.Q. Han, T.L. Lee, A. Tadich, D.C. Qi, L. Qiao, L. Chen, and K. H. L. Zhang (2019). Electronic structure and p -type conduction mechanism of spinel cobaltite oxide thin films, **115301**, 1.
[18] M. Satalkar, S. N. Kane (2016). On the study of Structural properties and Cation distribution of $Zn_{0.75-x}Ni_xMg_{0.15}Cu_{0.1}Fe_2O_4$ nano ferrite: Effect of Ni addition, *J. Phys. Conf. Ser.* **755**, 1.
[19] E. P. A. Couzijn, A. W. Ehlers, M. Schakel, K. Lammertsma (2006). Electronic Structure and Stability of Spinel Oxides **39**(S1), 251.
[20] C. G. Van De Walle, J. Neugebauer (2004). First-principles calculations for defects and impurities: Applications to III-nitrides, *J. Appl. Phys.* **95**(8), 3851.
[21] M. Lenglet, R. Guillamet, J. Dürr, D. Gryffroy, R. E. Vandenberghe (1990). Electronic structure of $NiCo_2O_4$ by XANES, EXAFS and 61Ni Mössbauer studies, *Solid State Commun.* **74**(10), 1035.
[22] K. Krezhov, P. Konstantinov (1997). Cationic distributions in the binary oxide spinels $M_xCo_{3-x}O_4$ (M=Mg,Cu,Zn,Ni), *Phys. B Condens. Matter* **234–236**, 157.
[23] C. Y. Ouyang, S. Q. Shi, M. S. Lei (2009). Jahn-Teller distortion and electronic structure of $LiMn_2O_4$, *J. Alloys Compd.* **474**(1–2), 370.
[24] X. Shi, S. L. Bernasek, A. Selloni (2016). Formation, electronic structure, and defects of Ni substituted spinel cobalt oxide: A DFT+U study, *J. Phys. Chem. C* **120**(27), 14892.
[25] J.F. Marco, J.R. Gancedo, M. Gracia, J.L. Gautier, E.I. Ríos, H.M. Palmer, C. Greaves, F.J. Berry. Cation distribution and magnetic structure of the ferrimagnetic spinel $NiCo_2O_4$, *J. Mater. Chem.* **11**(12), 3087.
[26] J. Chen, X. Wu, A. Selloni (2011). Electronic Structure and Bonding properties of cobalt oxide in the spinel structure, *Phys. Rev. B* **83**, 245204.

[27] A. Walsh, S.-H. Wei, Y. Yan, M. M. Al-Jassim, J. A. Turner (2007). Structural, magnetic, and electronic properties of the Co-Fe-Al oxide spinel system: Density-functional theory calculations, *Phys. Rev. B* **76**(16), 165119.
[28] S. Hirai, W.L. Mao, (2013). Novel pressure-induced phase transitions in Co3O4. Applied Physics Letters, **102**(4), 041912.
[29] F. Wang, L. Zhang, L. Xu, Z. Deng, W. Shi (2017). Low temperature CO oxidation and CH 4 combustion over Co 3 O 4 nanosheets, *Fuel* **203**, 419.
[30] A. Louardi, A. Rmili, F. Ouachtari, A. Bouaoud, B. Elidrissi, H. Erguig (2011). Characterization of cobalt oxide thin films prepared by a facile spray pyrolysis technique using perfume atomizer, *J. Alloys Compd.* **509**(37), 9183.
[31] L. Bai, M. Pravica, Y. Zhao, C. Park, Y. Meng, S.V. Sinogeikin, G. Shen (2012). Charge transfer in spinel Co3O4 at high pressures. *Journal of Physics: Condensed Matter* **24**(43), 435401.
[32] V. Stevanović, M. D'Avezac, A. Zunger (2010). Simple point-ion electrostatic model explains the cation distribution in spinel oxides, *Phys. Rev. Lett.* **105**(7), 11.
[33] Y. Li, P. Hasin, Y. Wu (2010). $Ni_xCo_{3-x}O_4$ nanowire arrays for electrocatalytic oxygen evolution, *Adv. Mater.* **22**(17), 1926.
[34] A. E. Merad, M. B. Kanoun, S. Goumri-Said (2006) Ab initio study of electronic structures and magnetism in ZnMnTe and CdMnTe diluted magnetic semiconductors, *J. Magn. Magn. Mater.* **302**(2), 536.